

OUTFLOWS IN SODIUM EXCESS OBJECTS

JONGWON PARK¹, HYUNJIN JEONG^{2,3}, AND SUKYOUNG K. YI¹

¹Department of Astronomy, Yonsei University, Seoul 120-749, Korea; yi@yonsei.ac.kr

²Korea Astronomy and Space Science Institute, Daejeon 305-348, Korea

³Korea University of Science and Technology, Daejeon 305-350, Korea

Draft version May 8, 2018

ABSTRACT

van Dokkum and Conroy revisited the unexpectedly strong Na I lines at 8200 Å found in some giant elliptical galaxies and interpreted it as evidence for unusually bottom-heavy initial mass function. Jeong et al. later found a large population of galaxies showing equally-extraordinary Na D doublet absorption lines at 5900 Å (Na D excess objects: NEOs) and showed that their origins can be different for different types of galaxies. While a Na D excess seems to be related with the interstellar medium (ISM) in late-type galaxies, smooth-looking early-type NEOs show little or no dust extinction and hence no compelling sign of ISM contributions. To further test this finding, we measured the doppler components in the Na D lines. We hypothesized that ISM would have a better (albeit not definite) chance of showing a blueshift doppler departure from the bulk of the stellar population due to outflow caused by either star formation or AGN activities. Many of the late-type NEOs clearly show blueshift in their Na D lines, which is consistent with the former interpretation that the Na D excess found in them is related with star formation-caused gas outflow. On the contrary, smooth-looking early-type NEOs do not show any notable doppler component, which is also consistent with the interpretation of Jeong et al. that the Na D excess in early-type NEOs is likely not related with ISM activities but is purely stellar in origin.

Subject headings: catalogs – galaxies: elliptical and lenticular, cD – galaxies: spiral – galaxies: abundances – galaxies: stellar content – galaxies: evolution

1. INTRODUCTION

The behavior of sodium spectral features has garnered much attention as it has become known that some galaxies show enhanced Na D doublet strengths at 5890 and 5896 Å and enhanced Na I doublet strengths at 8183 and 8195 Å. Numerous studies have been performed over the last three decades to understand these lines, but it is still unclear exactly how some galaxies exhibit a sodium excess.

Recent research focused on variation of an initial mass function (IMF) has provided an interesting possibility. The stellar IMF is usually considered a universal function, but the possibility of a non-universal IMF has been raised by several authors (see e.g. Davé 2008; van Dokkum 2008; Trager et al. 2000; Graves, Faber & Schiavon 2009; Treu et al. 2010; van Dokkum & Conroy 2010). In studies on the Ca II triplet at 8500 Å, Saglia et al. (2002) found an anti-correlation between the strength of the Ca II triplet region and the velocity dispersion for elliptical galaxies and concluded that bottom-heavy IMFs are favored (see also Cenarro et al. 2003). Recently, van Dokkum & Conroy (2010) reported observing a near-infrared Na I doublet in the spectra of massive early-type galaxies, and claimed that these excesses can be explained by a bottom-heavy IMF (see also van Dokkum & Conroy 2012). This implies that massive early-type galaxies should possess relatively more low-mass stars.

An alternative solution is also possible. It is well known that the Na D feature is sensitive to Na-enhancement ([Na/Fe]). The discovery of non-solar abundance patterns in early-type galaxies was first made by O’Connell (1976) and Peterson (1976). They found extreme en-

hancement of Mg *b* and Na D features with respect to calcium and iron peaks, and concluded that this was a result of higher metal abundance. Worthey (1998) also claimed that strong Na features are caused by an overabundance of [Na/Fe] (see also Worthey, Ingermann & Serven 2011). This is a trivial interpretation and thus not satisfying unless the origin for the enhancement is given clearly.

Furthermore, ISM could also increase the Na D line strength. Until the early 1980s it was thought that only late-type galaxies had significant ISM. Advances in X-ray and radio astronomy, however, have demonstrated that many early-type galaxies also have an unignorable amount of ISM. A direct method of measuring hydrogen gas column densities to detect ISM is possible via spectroscopy in the ultraviolet, because observations between 70 and 1000 Å are sensitive to small amounts of hydrogen and helium in the ISM. If it is not easy to obtain such data because of instrumental limitations; an alternative way is to use absorption lines such as K I, Ca II, and Na I in the more accessible optical region of the spectrum. The Na D absorption lines, especially, provides a good probe of cold ISM in the outflow. According to Chen et al. (2010), Na D absorption arises from cool gas in the disk and a blueshifted Na D absorption is frequently detected in star-forming galaxies (see also Heckman et al. 2000).

To understand the origin of the Na D excess, Jeong et al. (2013; J13 hereafter) explored the properties of Na D excess objects (NEOs) from the seventh data release of the Sloan Digital Sky Survey (SDSS; Abazajian et al. 2009), with morphological information obtained through visual inspection of galaxy images. They found

the use of bottom-heavy IMF not capable of reproducing the observed strength of Na D lines much but instead found it necessary to evoke an *ad hoc* enhancement of Na ($[\text{Na}/\text{Fe}] \sim 0.3$), just as in Worthey (1998). Their work does not necessarily rule out the possibility of a bottom-heavy IMF but hints that there is another missing physics that controls the Na D strengths more importantly (see also Yi & Jeong 2015). Indeed, weak lensing studies (Spiniello et al. 2012; Spiniello, Trager & Koopman 2015) suggest that a bottom-heavy IMF (similar to the original Salpeter IMF) helps reproducing the high values of mass derived on lensing galaxies, while the use of Na enhancement was additionally required.

Jeong et al. (2013) also found that little dust extinction seems present in smooth-looking *early-type* NEOs quoting the OSSY database (Oh et al. 2011), which supports the interpretation of stellar (rather than ISM) origin for the Na strength excess. As a further confirmation test, we hereby present the result of doppler measurement on the shape of NaD lines for the J13 samples of NEOs. If the NaD excess is related to ISM, we may detect doppler components in NaD line shapes due to gaseous outflows in actively star-forming galaxies (Chen et al. 2010) or active galactic nucleus (AGN) galaxies (Davis et al. 2012).

2. GALAXY SAMPLE

The parent sample for this study is the NEOs from J13. The J13 sample is drawn from the SDSS DR7 in the redshift range $0.00 \leq z \leq 0.08$ by applying an absolute *r*-band magnitude cut-off of -20.5 to obtain a volume-limited sample and signal-to-noise (S/N) cut-off of 20 to guarantee high quality spectroscopic data. To find NEOs, J13 defined a new index, $fNaD$, which quantifies the Na D excess as follows:

$$fNaD = \frac{\text{NaD (Observed)} - \text{NaD (Model)}}{\text{NaD (Model)}}, \quad (1)$$

where NaD (Observed) is the observed Na D line strength and NaD (Model) is the expected model NaD line strength. $fNaD \geq 0.5$ is used as a criterion for the NaD excess, and $0.0 \leq fNaD \leq 0.1$ is used to create a control sample. The sample galaxies were then morphologically classified via visual inspection. The NEOs were carefully assigned to four classes: (1) ordinary early-type galaxies (oETGs), (2) peculiar early-type galaxies (pETGs), (3) ordinary late-type galaxies (oLTGs), and (4) peculiar late-type galaxies (pLTGs). We note that galaxies with asymmetric features and dust patches (or lanes) are classified as peculiar types. In the case of control sample galaxies, these are simply divided into two categories: early-type galaxies (cETG) and late-type galaxies (cLTG). The details of the sample are described more fully in Section 2 of J13.

3. FITTING METHODOLOGY

As mentioned in Section 1, we assume that if NaD excess has ISM-origin, NaD absorption line would be blueshifted by the effect of outflow such as galactic superwind or AGN outflow. It is known that an NaD doublet is a good tracer of cold ISM in the outflow. In order to measure the doppler component, we tried both Gaussian and Voigt functions to fit each galaxy spectrum near

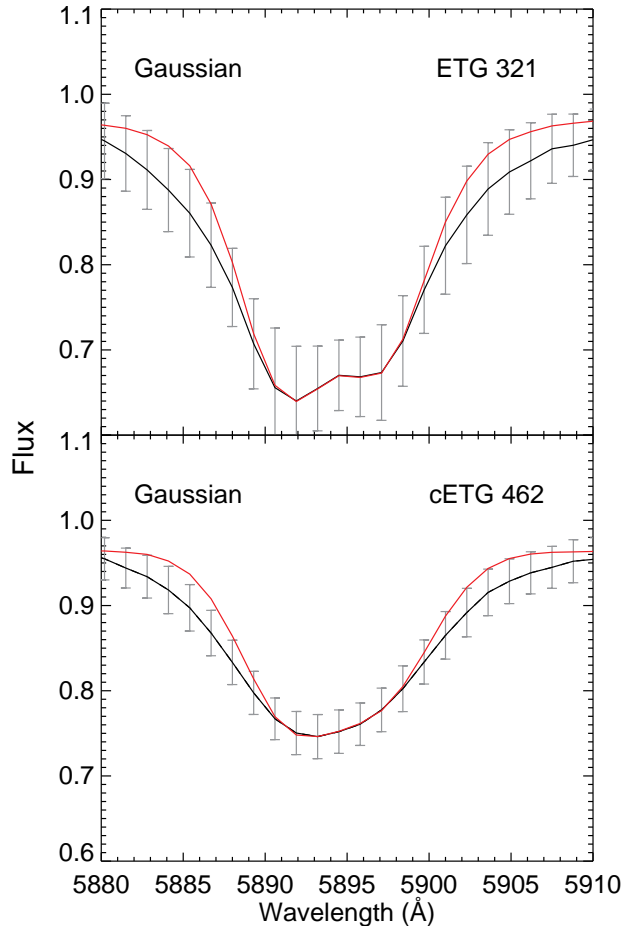


FIG. 1.— The stacked spectra of our early-type NEOs (top) and early-type control sample galaxies (bottom) from the SDSS database (black lines). Only the galaxies with good spectral fit ($\chi_r^2 \leq 3.0$) are shown here. The error bars indicate 1σ scatter in the sample. Red lines show the stacked SED of their corresponding fits.

the NaD absorption lines. Note that we fit the NaD line profile with two Gaussian (or Voigt) profiles. A possible criticism is that our fits are mainly mathematical rather than physical. However, it is the simplest method that can be used just to investigate whether NEOs show a blueshift doppler departure from the bulk of the stellar population or not.

3.1. Gaussian Fitting

We first adopted two Gaussian profiles to fit each galaxy spectrum and reproduce the shapes of the NaD doublet lines using the following formula:

$$y = a_1 \exp\left(-\frac{(x - \mu_1)^2}{2\sigma^2}\right) + a_2 \exp\left(-\frac{(x - \mu_2)^2}{2\sigma^2}\right), \quad (2)$$

where a and σ represent the line depth and width of the NaD absorption feature, respectively, and μ is the position of the centroid. For fitting, we assume that the line widths (σ) of the two Gaussian profiles are the same because they originated from the same galaxy, and two pseudo-continuum band-passes of NaD are identified as $[5860.625 - 5875.625 \text{ \AA}]$ and $[5922.125 - 5948.125 \text{ \AA}]$ from

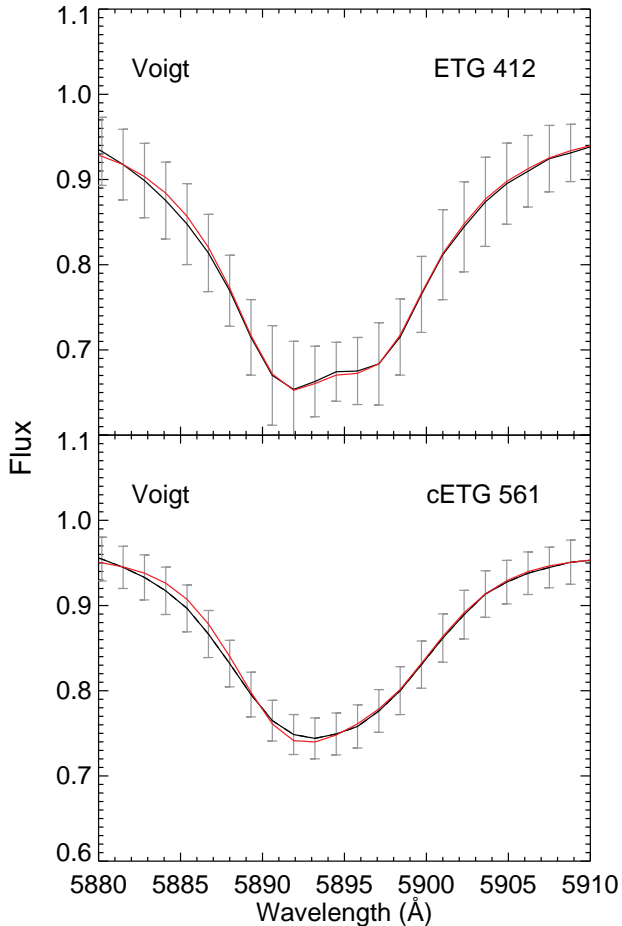


FIG. 2.— Same as Figure 1 but based on Voigt fitting. Note that Voigt profiles reproduce the shapes of the Na D lines much better.

Worthey, Faber & Gonzalez (1994). To measure the doppler components, the quality of our fits to the observed spectra is important. Therefore, we calculated a reduced χ^2 (χ_r^2) near the two dips, and only galaxies with $\chi_r^2 \leq 3.0$ are included in our final sample.

Figure 1 shows the observed stacked spectra (black solid lines) of early-type NEOs (ETG) and early-type control sample galaxies (cETG) in the Na D region. For comparison, we stacked their Gaussian fits (red solid lines). The models match the observed spectra well near the two dips, but there is a marked discrepancy in the fit on the sides (wings). One might be tempted to interpret this mismatch as an outflow effect, but if this interpretation is followed, then the same result in the early-type control sample is not explainable.

3.2. Voigt Fitting

Some lines like Ca II H and K, Ca I at 4227 Å, Na D, and Mg b show strong pressure-broadened wings in the spectra of cool stars. It is known that the Voigt profile is particularly well suited to fit the wings of such lines. The Voigt profile is defined by a convolution of the Gaussian and Lorentzian functions:

$$V(x) = k\tilde{V}(x), \quad (3)$$

$$\tilde{V}(x) = \frac{a\gamma}{\pi} \int_{-\infty}^{\infty} \frac{e^{-(x'-\mu)^2/2\sigma^2}}{(x-x')^2 + \gamma^2} dx', \quad (4)$$

where k is a/\tilde{V}_{max} , a and σ denote the depth and width of the Gaussian component, μ is the position of the centroid, and γ corresponds to the width of the Lorentzian component. The shape of the Voigt profile is highly sensitive to the value of γ , so we defined k as a/\tilde{V}_{max} to restrict the γ contribution to only the width of the wings. We then adopted two Voigt profiles to fit the Na D doublet for each galaxy spectrum, using the following form:

$$y = V_1(x) + V_2(x). \quad (5)$$

Observed stacked spectra (black solid lines) of early-type NEOs (ETG) and early-type control sample galaxies (cETG) with their stacked fits (red solid lines) obtained using two Voigt profiles are shown in Figure 2. Figures 1 and 2 show different numbers of galaxies mainly because they show only the galaxies for which χ_r^2 was achieved to be better than 3.0 while this cut depends on the fitting method. In addition, we excluded some fits even if chi squared was small when the fits required the positions of the fitting centroids to be farther than 0.5 Å from the pre-assumed positions of the doublets. Some displacement of centroids was allowed in the fitting procedure because of the limited spectral resolution and the uncertainty in redshift determination. Given that the result based on the Gaussian fitting shows a marked discrepancy in the fit (see Figure 1), the Voigt fitting reproduces the shapes of the Na D lines in a markedly better way, especially for the wings in the spectra. For a sanity check, the mean value of the width (dispersion) in the Gaussian component (σ in Equation 4) is $150 \pm 50 \text{ km s}^{-1}$, which roughly corresponds to the typical value of velocity dispersion of galaxies.

To compare the Gaussian and Voigt fitting methods, we show the fit residuals of our sample galaxies according to their morphologies in Figure 3. It should be noted that the fit residual based on the Voigt fitting method (solid lines) is below 1% except in the He I region at 5875 Å, while the Gaussian fitting method fails to reproduce the wings of Na D even for the control sample (see cETG and cLTG cases).

4. DISCUSSION

The broadening of absorption lines is difficult to interpret because the physics of the curve of growth is complex. Thus, we focus instead on the blueshift doppler departure from the bulk of the stellar population due to outflow caused by either star formation or AGN activity by measuring the centroids of the lines. As shown in Section 3, Voigt profiles provide conspicuously better fits to spectra, so we exploit results of Voigt profile fitting in our final analysis. To measure the doppler component of the Na D absorption lines, we define as follows:

$$\Delta\mu_1 = \mu_1 - 5891.6 \text{ Å}, \quad (6)$$

where μ_1 and 5891.6 are the left-dip positions of the best-fit for each galaxy and the Na D absorption lines in vacuum, respectively. If the line shows a blueshift doppler departure from the bulk of the stellar population, $\Delta\mu_1$ has a negative value.

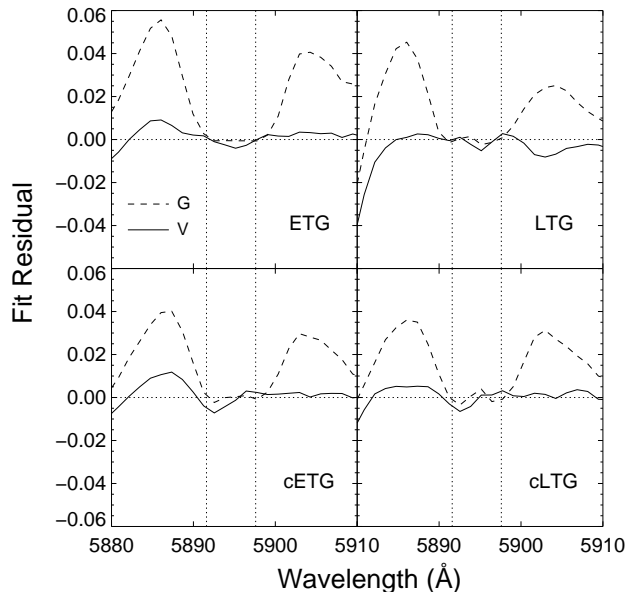


FIG. 3.— Stacked Gaussian (dashed lines) and Voigt (solid lines) fit residuals. Two dip positions of NaD are shown by vertical dotted lines.

Figure 4 presents the amount of NaD absorption line shift with respect to the NaD line strength. To investigate the dominant process that causes this outflow component, we use the BPT classification information from J13: star-forming (SF), composite (i.e., hosting both star formation and AGN activity, Co), Seyfert (Se), LINER (LI), or non-emission line galaxies (NE). Furthermore, the $\Delta\mu_1$ distributions of the control sample are shown in gray bands (panels g and h) for easy comparison. The key point in this investigation is to check whether the NEOs are so significantly different in the line shift compared with the control sample or not.

The left panels of Figure 4 show the early-type cases: ordinary (smooth-looking) early-type NEOs (oETG, a), peculiar (non-smooth) early-type NEOs (pETG, c), early-type NEOs (oETG + pETG, e), and early-type control sample (cETG, g). A cursory glance at this diagram shows that most early-type NEOs do not seem to show any particular blueshift of the NaD absorption lines. The fraction showing a shift bluer than those of the control counterparts ($\Delta\mu_1 \leq -0.6$) is roughly 4% (17/412, panel e). This result implies that ISM and dust are not likely the main factors causing the increase of the NaD line strength of early-type NEOs.

A possible criticism can be made by asking whether the non-shifted NaD absorption line provides direct evidence of non-ISM. It is known that there should also be a sign of dust extinction to allow neutral sodium to survive in the ISM. This implies that, if the NaD line strength of early-type NEOs is significantly enhanced through ISM effects, these galaxies are more likely to show a correlation between dust extinction and NaD line strength. However, J13 found that there was no correlation between the $E(B - V)$ values and f_{NaD} . On the contrary, the strongest early-type NEOs were the ones with the lowest dust extinction.

It is also worth noting that almost all of the ordinary early-type NEOs (oETGs, panel a) have overall ranges of

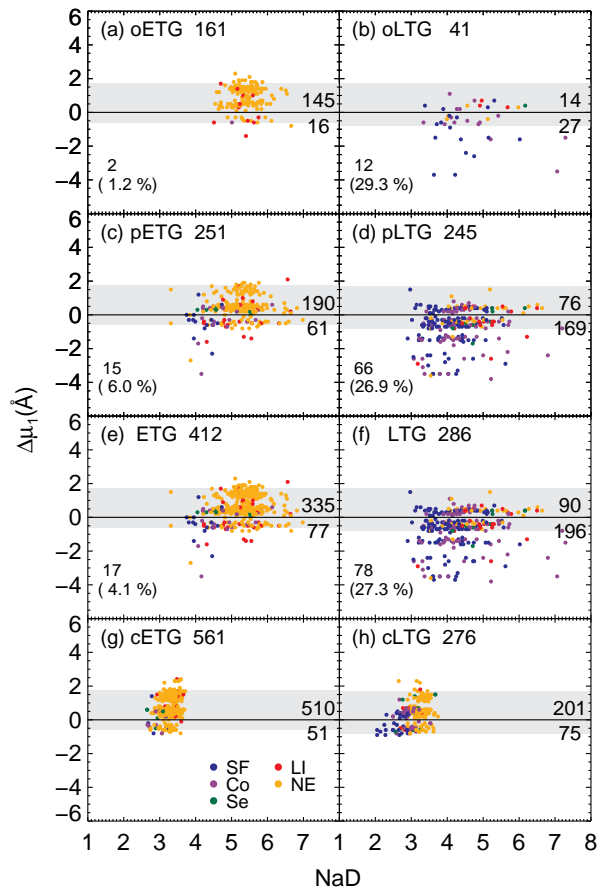


FIG. 4.— Amount of NaD absorption line shift with respect to NaD line strength. In each panel, the number of sample galaxies, the number of galaxies showing blue or redshift are given. Emission-line classification (based on the BPT diagnostic) is also given in different color. The gray band shows the range (encompassing the 95% of the sample) of doppler shift exhibited by the control sample in panels (g) and (h). For NEOs, the number and fraction of galaxies showing significantly blueshifted NaD absorption feature (below the bands) are shown in bottom left corner of each panel (from (a) to (f)). Note that the bulk of our sample galaxies show a systematic red shift by 0.6 \AA compared to the prediction from the vacuum experiment. We only focus on the difference between each sample and the control sample.

$\Delta\mu_1$ similar to those of the control sample (cETG, panel g). For example, the mean values of $\Delta\mu_1$ for oETG and cETG are 0.87 ± 0.68 and 0.78 ± 0.65 , respectively. However, one LINER AGN galaxy below the band is notable. If a galaxy reveals strong emission lines, this galaxy may be a gaseous system. So, there is the potential for this galaxy to show the NaD excess through ISM effects and to reveal a notable doppler component in NaD lines due to AGN-powered outflows. The physical mechanism by which an AGN could drive molecular gas out of a galaxy is still debated. Therefore, a detailed study of this galaxy using integral-field spectroscopy to constrain the outflow parameters and ionization mechanisms can shed light on the mechanism of gas expulsion from the galaxy and of quenching of star formation in early-type galaxies (Davis et al. 2012).

The right panels of Figure 4 show the late-type cases. In contrast to early-type NEOs, 27% of our late-type NEOs (78/286, LTG) clearly show blueshift in their NaD

lines in comparison with their control sample (cLTG). Furthermore, the overall distribution of late-type NEOs (panel f) is shifted toward more negative values than the distribution of the control sample (panel h). For example, the mean values of $\Delta\mu_1$ for LTG and cLTG are -0.64 ± 1.09 and 0.35 ± 0.68 , respectively. This strongly implies that these galaxies have an outflow component.

We checked the BPT classification for the 78 late-type NEOs with blueshifted NaD lines. Of 78, 41 and 30 galaxies are star-forming (SF) and composite (Co) galaxies, respectively, and only 5 galaxies are AGNs. Such findings suggest that the NaD excess found in these galaxies is related with star formation-caused gaseous outflows (galactic winds), which play an important role in the evolution of galaxies by removing/heating of cold gas in galaxies.

We thus conclude that early-type NEOs and late-type NEOs have completely different mechanisms underlying their NaD excess. Many late-type NEOs clearly show blueshift in their NaD lines, which means that their NaD

excess is related with ISM. On the other hand, early-type NEOs do not show any significant doppler component. While this does not necessarily rule out a possibility of ISM origin, it would be much more natural to conclude that their excessive NaD is of stellar origin. To facilitate follow-up observations of these exciting objects, we provide a catalog of the sample galaxies presented in this paper in Table 1.

ACKNOWLEDGMENTS

HJ acknowledges support from the Basic Science Research Program through the National Research Foundation of Korea (NRF), funded by the Ministry of Education (NRF-2013R1A6A3A04064993). SKY acknowledges support from the National Research Foundation of Korea (Doyak 2014003730). This study was performed under the DRC collaboration between Yonsei University and the Korea Astronomy and Space Science Institute.

REFERENCES

- Abazajian, K. N., Adelman-McCarthy, J. K., Agüeros, M. A., et al. 2009, *ApJS*, 182, 543
- Cenarro, A. J., Gorgas, J., Wvzekis, A., Cardiel, N., & Peletier, R. F. 2003, *MNRAS*, 339, L12
- Chen, Y., Tremonti, C. A., Heckman T. M., Kauffmann, G., & Weiner, B. J. 2010, *ApJ*, 140, 445
- Davé, R. 2008, *MNRAS*, 385, 147
- Davis, T., et al., 2012, *MNRAS*, 426, 1574
- Graves, G. J., Faber, S. M., & Schiavon, R. P. 2009, *ApJ*, 698, 1590
- Heckman, T. M., Lehnert, M. D., Strickland, D. K., & Armus, L. 2000, *ApJS*, 129, 493
- Jeong, H., Yi, S. K., Kyeong, J., Sarzi, M., Sung, E. -C., Oh, K. 2013, *ApJS*, 208, 7
- O'Connell R. W. 1976, *ApJ*, 206, 370
- Oh, K., Sarzi, M., Schawinski, K., & Yi, S. K. 2011, *ApJS*, 195, 130
- Saglia, R. P., Maraston, C., Thomas, D., Bender, R., & Colless, M. 2002, *ApJL*, 579, L13
- Spiniello, C., Trager, S. C., Koopmans, L. V. C., & Chen, Y. P. 2012, *ApJL*, 753, L32
- Spiniello, C., Trager, S. C., & Koopmans, L. V. C. 2015, *ApJ*, 803, 87
- Peterson, R. C. 1976, *ApJL*, 210, 123
- Trager, S. C., Faber, S. M., Worthey, G., & González, J. J. 2000, *AJ*, 120, 165
- Treu, T., et al. 2010, *ApJ*, 709, 1195
- van Dokkum, P. G. 2008, *ApJ*, 674, 29
- van Dokkum, P. G., & Conroy, C. 2010, *Nature*, 468, 940
- van Dokkum, P. G., & Conroy, C. 2012, *ApJ*, 747, 69
- Worthey, G. 1998, *PASP*, 110, 888
- Worthey, G., Faber, S. M., & González, J. J. 1994, *ApJ*, 94, 687
- Worthey, G., Ingermann, B. A., & Serven, J. 2011, *ApJ*, 729, 148
- Yi, S.K., & Jeong, H. 2015, in *Proc. IAU Symp. 311, Galaxy Masses as Constraints of Formation Models*, ed. M. Cappellari & S. Courteau (Cambridge Univ. Press: Cambridge), 69

TABLE 1
A SAMPLE OF THE CATALOGUE OF Na D EXCESS OBJECTS.

SDSS object id	$fNaD$	Na D ^a (Å)	Morphology	BPT class ^b	a1 ^c	a2 ^c	μ_1 ^d (Å)	μ_2 ^e (Å)	σ ^f (Å)	γ ^g	χ_r^2
(1)	(7)	(8)	(15)	(16)	(17)	(18)	(19)	(20)	(21)	(22)	(23)
587727179531354122	0.53	4.65	oETG	Quiescent	0.32	0.24	5892.8	5898.5	1.0	2.3	0.9
588009365862285317	0.53	4.76	pETG	LINER	0.20	0.19	5891.1	5897.3	2.7	3.0	0.8
587727179528339473	0.74	4.96	oLTG	LINER	0.31	0.28	5892.3	5898.3	1.5	2.3	1.9
587737827826204741	0.94	4.04	pLTG	Star-forming	0.21	0.16	5889.0	5894.9	2.3	3.3	1.9

Notes.

^aObserved line strength.

^bEmission line classification.

^cDepth of Gaussian component.

^dCentroid of the left Gaussian component.

^eCentroid of the right Gaussian component.

^fStandard deviation of Gaussian component.

^gHalf the FWHM of Lorentzian component.